Modifications of the Mesoscopic Structure of Cellulose in Paper Degradation

Mauro Missori,[1,*] Claudia Mondelli,[2] Marco De Spirito,[3] Carlo Castellano,[4] Marina Bicchieri,[1] Ralf Schweins,[5] Giuseppe Arcovito,[3] Massimiliano Papi,[3] and Agostina Congiu Castellano[4]

[1]*Istituto Centrale per la Patologia del Libro, Ministero per i Beni e le Attivitá Culturali, via Milano 76, I-00184 Rome, Italy*
[2]*Institut Laue Langevin 6, CNR-INFM and CRS Soft, Rue Jules Horowitz, F-38042 Grenoble Cedex 9, France*
[3]*Istituto di Fisica, Universitá Cattolica Sacro Cuore, Largo Francesco Vito 1, I-00168 Rome, Italy*
[4]*Dipartimento di Fisica, Universitá di Roma "La Sapienza," Piazzale Aldo Moro 2, I-00185 Rome, Italy*
[5]*LSS Group, ILL, 6 rue Jules Horowitz, F-38042 Grenoble Cedex 9, France*

(Received 6 March 2006; published 6 December 2006)

Paper is the main component of a huge quantity of cultural heritage. It is primarily composed of cellulose that undergoes significant degradation with the passage of time. By using small angle neutron scattering (SANS), we investigated cellulose's supramolecular structure, which allows access to degradation agents, in ancient and modern samples. For the first time, SANS data were interpreted in terms of water-filled pores, with their sizes increasing from 1.61 nm up to 1.97 nm in natural and artificially aged papers. The protective effect of gelatine sizing was also observed.

DOI: 10.1103/PhysRevLett.97.238001 PACS numbers: 81.05.Lg, 28.20.Cz

Paper has been the most widely used writing support since the Middle Ages [1], with the result that for centuries a growing number of books, documents, and artistic drawings has been accumulating in libraries, archives, and museums all over the world. The preservation of these cultural properties poses a significant challenge: that of limiting the deterioration of the paper materials found in them. An advanced knowledge of the microscopical characteristics of paper materials and their degradation processes is indispensable in order to fulfill this objective.

Paper sheets are primarily composed of a web of natural fibers of cellulose and other substances. In ancient times paper was produced from linen, hemp, and cotton rags impregnated with sizing material (i.e., gelatine), sometimes with fillers added [2]. Cellulose is a composite (crystalline/amorphous) material composed of a linear homopolysaccharide made up of repeating units of β-(1,4)-glucopyranose.

Hydrogen bonding between cellulose polymers is the principal mechanism responsible for cellulose's supramolecular structure, which in turn is made up of an assembly of crystalline domains and amorphous regions. In the case of flax and cotton, the crystalline domains have dimensions of 2–4 nm in cross section and 100 nm in length, while cellulose polymers measure 0.54 nm along the $10\bar{1}$ crystallographic axis [3].

The process of paper degradation has been modeled as a combination of cellulose acidic hydrolysis and oxidation [3,4]. Hydrolysis shortens the cellulose polymeric chains while oxidation causes the formation of carbonyl groups, the opening of glucopyranose rings and the shortening of polymeric chains. Oxidation is also responsible for discoloration, since the oxidized groups absorb even violet and blue light components [5]. Hydrolysis and oxidation are enhanced by the presence of environmental moisture selectively sorbed, in the accessible regions, by the cellulose substrate's hydrogen bonds [3,6]. Recently, water domains of radius 1.4–1.5 nm permeating the amorphous regions of cellulose microfibrils have been found by NMR spectroscopy [7].

Small angle neutron scattering (SANS) and x-ray scattering have already been used to investigate the supramolecular structure of modern paper and cellulose fibers [8]. Hydrogen-deuterium exchange from D_2O liquid or vapor phase, allowing the formation of heavy water clusters, was employed to modulate the scattering contrast [3,6,9]. In the previous scattering experiments on paper, however, scattering data were interpreted in terms of cellulose microfibrils only, without taking into account any possible contribution coming from water confined in pores at mesoscopic length scales, as suggested by the NMR experiments. In this Letter we demonstrate the feasibility of using SANS to detect water-filled pores in cellulose and measuring the increasing dimensions of water domains in paper as it undergoes degradation.

Modern samples of Whatman No. 1 (W4) and Fabriano-Perusia papers (F5, F6) (see Table I) were artificial aged in a climatic chamber for 28 days at 80 °C and 65% rH in dark conditions, according to the ISO 5630-3:1986 standard. Ancient unprinted specimens consist of small pieces of dated and identified paper, presenting various levels of degradation and discoloration, produced during the 15th century in European countries. All samples, with the exception of W4, were sized with gelatine, as was customary in ancient times to improve the paper's writing quality [2,10].

Three sets of specimens were created by cutting 3 adjacent pieces (1×2.5 cm^2 each) from each paper sample. Hydrated samples (H series) were left to equilibrate (2 h) in an H_2O saturated atmosphere, and then sealed in Hellma quarz cuvettes. The time needed to reach water-paper equilibrium was tested in advance, and found to be less

TABLE I. List and description of the specimens measured in the experiment. PC1 values result from the principal component analysis of optical spectra. Degradation increases by decreasing PC1 [5].

Sample label	Sample description	Fiber composition	Aging conditions or state of degradation	PC1 value	R_g (nm)
F6	Fabriano-Perusia, 1950	22% cotton/78% cotton linters	Not artificially aged		1.61 ± 0.04
F5	Fabriano-Perusia, 1950	22% cotton/78% cotton linters	Artificially aged		1.67 ± 0.04
W4	Whatman No. 1	Cotton	Artificially aged		1.84 ± 0.05
M3	Milan, 1430	Cotton/linen	Good	14.13	1.85 ± 0.07
P7	Perpignan, 1413	Linen	Intermediate	7.00	1.95 ± 0.04
M2	Milan, 1430	Cotton/linen	Bad	4.96	1.97 ± 0.03
N1	Nuremberg, 15th century	Linen	Very bad	−14.91	1.97 ± 0.08

than 1 h. Fully deuterated (D series) and partially deuterated (HD series) samples were first dried in a N_2 atmosphere for 2 h and successively left to equilibrate (2 h) in a D_2O and a $50\%H_2O/50\%D_2O$ mixture saturated atmosphere, respectively, and then sealed in Hellma quarz cuvettes.

Measurements were performed on the SANS Instrument D11 at Institut Laue-Langevin in Grenoble, France. Scattering intensities were recorded by a two-dimensional position-sensitive ^{3}He detector. Three different instrument settings were used corresponding to a momentum transfer range $q = 4\pi/\lambda \sin(\vartheta/2)$ of $0.0018 < q < 0.21$ Å^{-1}. H_2O was used for instrumental calibration. The differential scattering cross sections per unit volume of the paper samples were obtained by applying the standard normalization and correction procedures [11].

In Fig. 1 we report the neutron scattering profiles for all the samples of D series. All the curves share a common behavior: a low q decay followed by a roll-off at higher q, which minutely, but continuously, shifts toward higher values of q with the increase of artificial or natural paper aging. In the cases of H and HD series (an example is shown in the upper inset of Fig. 2 for sample F6), similar behavior has been observed, although with a less pronounced shoulder, which almost disappeared in the case of the HD samples. Therefore the shoulder may be due to constructive interference from a repeat structure produced by intercalation of water between cellulose microfibrils. Indeed, at these length scales (of a few nanometers), water is locally constrained in clusters or pools instead [7]. These water clusters, acting as strong scatterers, provide a non-negligible scattering contribution.

Let us picture, at the length scales investigated in the present work, paper as a two phases system [12]: one constituted of cellulose arranged in various supramolecular

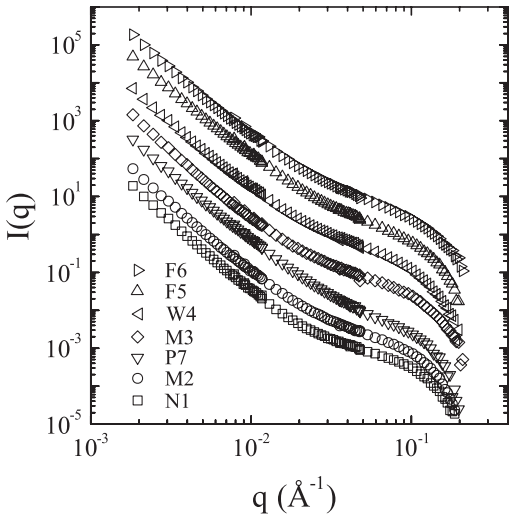

FIG. 1. Neutron scattering intensity versus scattering vector q from all the samples exposed to D_2O atmosphere (listed in Table I) are reported. Curves are arbitrarily shifted for clarity.

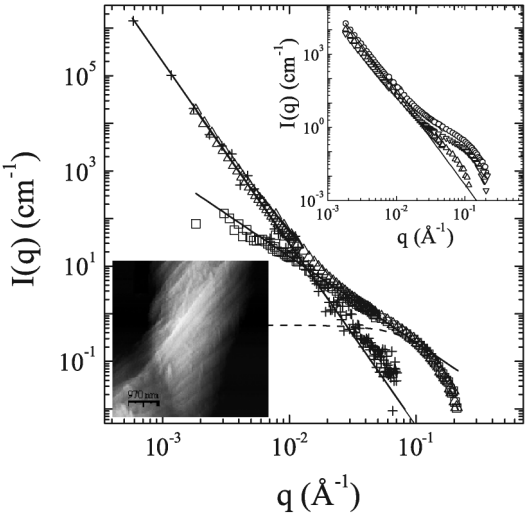

FIG. 2. The SANS scattering intensity profiles (open triangles) and that obtained from AFM image analysis (crosses) from the $F6_D$ sample. The data curve with open squares is the difference between the SANS curve and the low q background. Guinier (dashed line) and a fractal (continuous line) least-squares fits are also included. In the upper inset SANS profiles from samples $F6_D$ (circles), $F6_H$ (downwards triangles), and $F6_{HD}$ (upward triangles) are also reported. The dotted line is the nonlinear square fitting with a power law in the low q region. In the lower inset an AFM image of a single fiber from $F6_D$ is reported.

structures (fibers), and the other made up of voids or pores filled with water, which are formed by the nonideality of packing of the cellulose polymers (amorphous region). In the pores phase, which is accessible to external agents (i.e., water), it is possible to adjust the contrast by altering the proportion of H_2O to D_2O to match or exceed that of the other selected phase (see upper inset of Fig. 2). Moreover, the minute but continuous shift of the shoulder toward higher values of q with increasing artificial or natural aging of paper suggests that it is correlated to structural modifications induced by the degradation.

Since cellulose fiber sizes (ranging from 2 nm up to ~ 10 μm in radius R) [3] are larger than the pore sizes (~ 1.5 nm) [7], the low q region (i.e., before the shoulder) of the scattering profile should be dominated by the cellulose polymer phase.

Under such an assumption and since the transferred momentum results are much larger than the reciprocal of the fiber size ($qR \gg 1$), the Porod law ($I = Aq^{-d_s}$) applies to this q region and captures experimental data (continuous line in Fig. 2). The value of the exponent $d_{s(\mathrm{SANS})}$ (the fractal surface dimension), obtained by averaging samples $F6_H$, $F6_D$, and $F6_{HD}$, is equal to 3.8 ± 0.2. Conversely, the amplitude A grows with the scattering cross section of the sorbed isotope adopted, suggesting that this scattering contribution is superimposed on that deriving from sorbed isotopes homogeneously distributed in between the fibers.

To strengthen this assumption images of sample $F6_D$ have been also collected by using atomic force microscopy (AFM) in tapping mode [13]. The rough surface of a cellulose fiber composed of an assembly of oriented fibrils (see lower inset of Fig. 2) can be quantitatively analyzed by performing the power spectral density (PSD) (i.e., the square of the magnitude of the Fourier transform of the surface profile) along the fiber cross section. Since PSD, which depends on the fibril form factor $S(q)$, is proportional to the scattered intensity [$I(q) \sim S(q) = \sqrt{\mathrm{PSD}/q^5}$], we can directly compare AFM and SANS data (Fig. 2) [14]. AFM data (crosses), perfectly overlaping SANS data (open triangles) in the low q range, follow the Porod behavior, characterized by the exponent $d_{s(\mathrm{AFM})} = 3.81 \pm 0.02$ well in agreement with that obtained by SANS.

Finally, the extension to larger q values, with respect to SANS data, of the Porod behavior is noteworthy, since AFM techniques sensitive to the cellulose fibrils surface but not to embedded water allow us to definitely establish the presence of the two phases. Accordingly, the water clusters' scattering can easily be isolated by subtracting those arising from the cellulose polymer phase [15]. The resulting curve for the sample $F6_D$ (open squares), shown as an example, is reported together with the original one (open triangles) in Fig. 2. The new curve shows a power law decay in the intermediate q region of the probed wave vector up to a roll-off at higher q, after which a more rapid decay is observed. From this last decay the pores' mean sizes, proportional to q^{-1} in this q region, can be determined according to the Guinier approximation for spherical scatterers ($I(q) = I(0)/[1 + (qR_g)^2/3]^2$) [16]. To optimize the parameters estimation, we applied an iterative procedure called point perturbation analysis [17], which allows one to disclose systematic trends. Indeed, this fitting procedure, consisting in the iterative construction of a weighting profile, by lowering the weight to all those data points that do not belong to the model adopted (Guinier), allows for a significant increase of the number of data points considered in the fitting procedure. The best fit gives a mean radius $R_g = 1.61 \pm 0.04$ nm (dashed line in Fig. 2), a value well in agreement with previous NMR results, even if obtained on linters cellulose conditioned at 50% rH.

The spatial distribution of the above scatterers also contributes to the low q scattering intensity [18]. In the case of scatterers, fractally distributed in space, a power law decay of the scattered intensity ($I = \alpha q^{-D_m}$) is expected [18]. In our case, the fractal distribution of the water pools inside the fibers, recovered from a best fit, is characterized by a fractal dimension $D_m = 1.8 \pm 0.1$ (continuous line in Fig. 2).

The intensity profile of SANS data for all samples shows a behavior similar to that observed in sample F6 (Fig. 1), and the same data analysis has been adopted to establish water cluster sizes. To give greater emphasis to our results, let us organize the samples into three classes: ancient samples (N1, M2, M3, and P7), artificially aged samples (W4 and F5), and the modern sample (F6). Accordingly, the value of R_g, reported in Fig. 3 and Table I, appears clearly related to naturally or artificially aged paper ranging from 1.61 nm in the case of the modern paper to 1.97 nm for the most degraded specimen investigated.

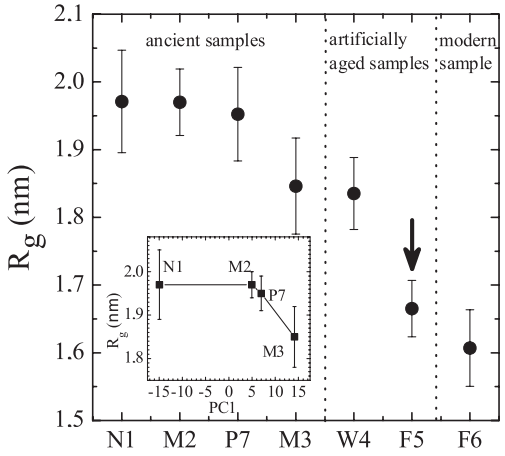

FIG. 3. The mean radius of the pore sizes for samples investigated is reported. In the inset, R_g of the ancient samples are plotted versus their PC1 values as obtained by optical spectroscopy. Degradation increases by decreasing PC1 [5].

Interestingly specimens F5 and W4, although undergoing the same artificial aging procedure, show clear evidence of the differences between their pore sizes (see Fig. 3) implying a lower degradation of sample F5 as compared to sample W4. Recalling that the F5 sample is gelatine sized, this result reinforces the hypothesis that gelatine, acting as a barrier and as a sacrificial layer, is a protective factor against environmental agents responsible for cellulose degradation in paper [2,10].

Finally, we would also relate the pore size to the papers' discoloration, which is connected to the presence of oxided groups in cellulose through the first principal component (PC1) of principal component analysis of optical reflectance spectra [5]. Even in this case a clear relation between the R_g of each ancient specimen and the PC1 appears (see inset of Fig. 3).

In conclusion, a new contribution to SANS from cellulose fibers has for the first time been analyzed and interpreted. We propose that the neutrons scattering curves of ancient and modern papers are due to the superimposition of at least two contributions: (i) the expected scattering from the cellulose fibers' surfaces and (ii) the scattering from the distribution of water clusters confined to pores at a mesoscopic level.

The relevance of such microdomains is very clear. Indeed, since their sizes increase with the natural or artificial aging of samples, it turned out that microscopical details of the cellulose fibers are a quantitative indicator of a paper's degradation. Our interpretation of this trend is that there is more interfacial area between the microfibers and water phases, which corresponds to an increasing number of exposed hydroxyl groups of polysaccharides. This implies that as the aging increases, the consolidated polymer structure is disrupted, with water overcoming some of the hydrogen bonding between adjacent polymer chains in the disordered regions. In addition, paper degradation can be prevented by sizing the sample with a protective agent (i.e., gelatine), which limits access to cellulose. Finally, for the first time, macroscopically observed degree of degradation in paper (i.e., discoloration) has been directly related to a mesostructural parameter (i.e., water-filled pore size).

We gratefully acknowledge Dr. M. Righini and Dr. A.-L. Dupont for their helpful suggestions. This research was also supported in part (M. D. S.) by the Universitá Cattolica del Sacro Cuore, Roma, Italy.

*Electronic address: mauro.missori@beniculturali.it

[1] D. Hunter, *Papermaking. The History and Technique of an Ancient Craft* (Cresset, London, 1957).
[2] G. Righini, A. L. Segre, G. Mattogno, C. Federici, and P. F. Munafo, Naturwissenschaften **85**, 171 (1998).
[3] H. Kraessig, *Cellulose. Structure, Accessibility and Reactivity Polymer Monographs* (Gordon and Breach, Singapore, 1993), Vol. 11.
[4] M. Strlic, J. Kolenc, J. Kolar, and B. Pihlar, J. Chromatogr. A **964**, 47 (2002).
[5] M. Missori, M. Righini, and S. Selci, Opt. Commun. **231**, 99 (2004).
[6] M. Mueller, C. Czihak, H. Schober, Y. Nishiyama, and G. Vogl, Macromolecules **33**, 1834 (2000).
[7] D. Capitani, N. Proietti, F. Ziarelli, and A. L. Segre, Macromolecules **35**, 5536 (2002).
[8] C. J. Garvey, I. H. Parker, R. B. Knott, and G. P. Simon, Holzforschung **58**, 473 (2004).
[9] J. Higgins and H. Benoit, *Polymers and Neutron Scattering* (Clarendon Press, Oxford, 1994).
[10] M. Missori, M. Righini, and A.-L. Dupont, Opt. Commun. **263**, 289 (2006).
[11] P. Lindner, in *Neutrons, X-Rays and Light: Scattering Methods Applied to Soft Condensed Matter*, edited by P. Lindner and Th. Zemb (Elsevier, Amsterdam, 2002).
[12] O. Glatter and O. Kratky, *Small Angle X-Ray Scattering* (Academic, London, 1982).
[13] M. Papi, G. Arcovito, M. De Spirito, M. Vassalli, and B. Tiribilli, Appl. Phys. Lett. **88**, 194102 (2006).
[14] J. Erlebacher *et al.*, Phys. Rev. Lett. **82**, 2330 (1999).
[15] A. Braun, F. E. Huggins, S. Seifert, J. Ilavsky, N. Shah, K. E. Kelly, A. Sarofim, and G. P. Huffman, Combust. Flame **137**, 63 (2004).
[16] A. Guinier and G. Fournet, *Small-Angle Scattering of X-Rays* (John Wiley and Sons, New York, 1955).
[17] E. Di Cera, F. Andreasi Bassi, and G. Arcovito, Phys. Lett. A **152**, 315 (1991).
[18] D. W. Schaefer and K. D. Keefer, Phys. Rev. Lett. **56**, 2199 (1986).